Chiroptical Switching Polyguanidine Synthesized by Helix-Sense-Selective Polymerization Using [(R)-3,3‘-Dibromo-2,2‘-binaphthoxy](di- tert -butoxy)titanium(IV) Catalyst

ARTICLE *in* JOURNAL OF THE AMERICAN CHEMICAL SOCIETY · MARCH 2005

Impact Factor: 12.11 · DOI: 10.1021/ja0453533 · Source: PubMed

3 AUTHORS, INCLUDING:

Bruce Novak
University of Texas at Dallas
135 PUBLICATIONS **5,641** CITATIONS

SEE PROFILE

J|A|C|S
ARTICLES
Published on Web 01/28/2005

Chiroptical Switching Polyguanidine Synthesized by Helix-Sense-Selective Polymerization Using [(*R*)-3,3′-Dibromo-2,2′-binaphthoxy](di-*tert*-butoxy)titanium(IV) Catalyst

Hong-Zhi Tang, Paul D. Boyle, and Bruce M. Novak*

Contribution from the Department of Chemistry, North Carolina State University, Raleigh, North Carolina 27695

Received August 2, 2004; Revised Manuscript Received December 13, 2004; E-mail: novak@chemdept.chem.ncsu.edu

Abstract: A series of chiral binaphthyl titanium alkoxide complexes were synthesized. Among them, chiral titanium complex [(*R*)-3,3′-dibromo-2,2′-binaphthoxy](di-*tert*-butoxy)titanium(IV) (**R-3**) exists as a crystallographic C_2 dimer in the solid state but a monomer in solution at room temperature. Application of **R-3** in the helix-sense-selective polymerization of achiral carbodiimide, *N*-(1-anthryl)-*N*′-octadecylcarbodiimide (**1**), yielded a well-defined regioregular, stereoregular poly[*N*-(1-anthryl)-*N*′-octadecylguanidine] (poly-**1b**) with a relatively narrow polymer dispersity index of 2.7. Full racemization of poly-**1b** at +80 °C in toluene requires more than 100 h. Interestingly, poly-**1b** was found to undergo fast reversible chiroptical switching at +38.5 °C in toluene. Furthermore, at room temperature, poly-**1b** shows a positively signed Cotton effect in toluene, but negative ones in THF and chloroform, respectively. The chiroptical switching takes place around the toluene content of 90% (vol) in the mixed toluene/THF solvents. This is the first example of chiroptical switching phenomenon occurring in a helical polymer possessing no chiral moieties in the polymer chains. We believe this reversible chiroptical switching phenomenon occurs by reorientation of anthracene rings relative to the chain director.

Introduction

Controlling and switching the chiroptical properties of (macro)molecules is of continued interest because of potential applications in sensor data storage, optical devices, and liquid crystalline displays.[1−6] Chiroptical switch can be controlled by temperature,[2] solvent,[3] additives,[4] irradiation,[5] and electron redox,[6] with thermo-driven chiroptical switching polymers being the most extensively studied. Examples include poly(L-aspartate β-esters),[2a,b] polyisocyanates,[2c−e] polysilanes,[1d,2f−i] and polyacetylenes.[2j−m] Solvent-driven chiroptical switching has been reported for poly(L-aspartate β-esters)[2a,3b,c] and poly(propiolic esters).[2l] To date, however, all chiroptical switching polymers are synthesized from chiral monomers, possessing stereo centers in the main or side chains. Herein, we wish to report the first chiroptical switching polymer (poly[*N*-(1-anthryl)-*N*′-octadecylguanidine], poly-**1b**, see Scheme 2), which possesses no chiral moieties in polymer chains. Poly-**1b** is synthesized by a highly regioregular, stereoregular, helix-sense-selective polymerization.

The helix-sense-selective polymerization of achiral monomers using chiral catalysts or chiral solvents yields kinetically controlled helical polymers, e.g., polyisocyanides,[7a−c] poly(quinoxaline-2,3-diyl)s,[7d,e] poly(trityl methacrylates),[1b,7f−h] poly(trityl methacylamides),[7i] polyacetylenes,[7j] and polyisocyanates.[7k]

(1) Typical reviews: (a) Hill, D. J.; Mio, M. J.; Prince, R. B.; Hughes, T. S.; Moore, J. S. *Chem. Rev.* **2001**, *101*, 3893. (b) Okamoto, Y.; Nakano, T. *Chem. Rev.* **1994**, *94*, 349. (c) Pu, L. *Acta Polym.* **1997**, *48*, 116. (d) Fujiki, M. *J. Organomet. Chem.* **2003**, *685*, 15.

(2) For poly(L-aspartate β-esters): (a) Bradbury, E. M.; Carpenter, B. G.; Goldman, H. *Biopolymers* **1968**, *6*, 837. (b) Watanabe, J.; Okamoto, S.; Satoh, K.; Sakajiri, K.; Furuya, H.; Abe, A. *Macromolecules* **1996**, *29*, 7084. For polyisocyanates: (c) Maeda, K.; Okamoto, Y. *Macromolecules* **1999**, *32*, 974. (d) Cheon, K. S.; Selinger, J. V.; Green, M. M. *Angew. Chem., Int. Ed.* **2000**, *39*, 1482. (e) Tang, K.; Green, M. M.; Choen, K. S.; Selinger, J. V.; Garetz, B. A. *J. Am. Chem. Soc.* **2003**, *125*, 7313. For polysilylenes: (f) Fujiki, M. *J. Am. Chem. Soc.* **2000**, *122*, 3336. (g) Fujiki, M.; Tang, H.-Z.; Motonaga, M.; Torimitsu, K.; Koe, J. R.; Watanabe, J.; Sato, T.; Teramoto, A. *Silicon Chem.* **2002**, *1*, 67. (h) Fujiki, M.; Koe, J. R.; Motonaga, M.; Nakashima, H.; Terao, K.; Teramoto, A. *J. Am. Chem. Soc.* **2001**, *123*, 6253. (i) Teramoto, A.; Terao, K.; Terao, Y.; Nakashima, H.; Sato, T.; Fujiki, M. *J. Am. Chem. Soc.* **2001**, *123*, 12303. For polyacetylenes: (j) Tabei, J.; Nomura, R.; Sanda, F.; Masuda, T. *Macromolecules* **2004**, *37*, 1175. (k) Cheuk, K. K. L.; Lam, J. W. Y.; Lai, L. M.; Dong, Y.; Tang, B. Z. *Macromolecules* **2003**, *36*, 9752. (l) Nakako, H.; Nomura, R.; Masuda, T. *Macromolecules* **2001**, *34*, 1496. (m) Tabei, J.; Nomura, R.; Masuda, T. *Macromolecules* **2003**, *36*, 573. (n) Yashima, E.; Maeda, K.; Sato, O. *J. Am. Chem. Soc.* **2001**, *123*, 8159.

(3) (a) Khatri, C. A.; Pavlova, Y.; Green, M. M.; Morawetz, H. *J. Am. Chem. Soc.* **1997**, *119*, 6991. (b) Bradbury, E. M.; Carpenter, B. G.; Robinson, C. C.; Goldman, H. *Macromolecules* **1971**, *4*, 557. (c) Toniolo, C.; Falxa, M. L.; Goodman, M. *Biopolymers* **1968**, *6*, 1579.

(4) (a) Novak, B. M.; Schlitzer, D. S. *J. Am. Chem. Soc.* **1998**, *120*, 2196. (b) Yashima, E.; Maeda, K.; Okamoto, Y. *Nature* **1999**, *399*, 449. (c) Ishikawa, M.; Maeda, K.; Mitsutsuji, Y.; Yashima, E. *J. Am. Chem. Soc.* **2004**, *126*, 732. (d) Miyake, H.; Yoshida, K.; Sugimoto, H.; Tsukube, H. *J. Am. Chem. Soc.* **2004**, *126*, 6524. (e) Su, S.-J.; Takeishi, M.; Kuramoto, N. *Macromolecules* **2002**, *35*, 5752. (f) Berl, V.; Huc, I.; Khoury, R. G.; Krische, M. J.; Lehn, J.-M. *Nature* **2000**, *407*, 720.

(5) (a) Koumura, N.; Zijlstra, R. W. J.; van Delden, R. A.; Harada, N.; Feringa, B. L. *Nature* **1999**, *401*, 152. (b) Huck, N. P. M.; Jager, W. F.; de Lange, B.; Feringa, B. L. *Science* **1996**, *273*, 1686. (c) Janicki, S. Z.; Schuster, G. B. *J. Am. Chem. Soc.* **1995**, *117*, 8524. (d) Mayer, S.; Maxein, G.; Zental, R. *Macromolecules* **1998**, *31*, 8522. (e) Muller, M.; Zentel, R. *Macromolecules* **1994**, *27*, 4404. (f) Maxein, G.; Zentel, R. *Macromolecules* **1995**, *28*, 8438. (g) Muller, M.; R. Zentel *Macromolecules* **1996**, *29*, 1609. (h) Mayer, S.; Zentel, R. *Macromol. Chem. Phys.* **1998**, *199*, 1675.

(6) (a) Zahn, S.; Canary, J. W. *Science* **2000**, *288*, 1404. (b) Zahn, S.; Canary, J. W. *Trends Biotechnol.* **2001**, *19*, 251.

10.1021/ja0453533 CCC: $30.25

Scheme 1

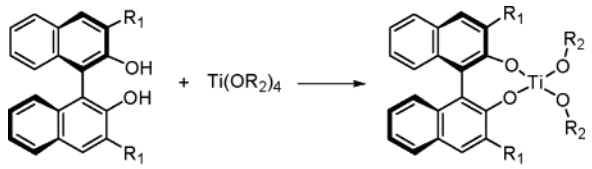

L1 ~ L6 **R-I ~ R-XII**

R_1	Ligand	R_2	Catalyst	Existing form
-H	**L1**	^{i}Pr	**R-1**	Aggregated
-H	**L1**	^{t}Bu	**R-2**	Aggregated
-Br	**L2**	^{t}Bu	**R-3**	Monomeric
-$SiMe_3$	**L3**	^{i}Pr	**R-4**	Aggregated
-$SiMe_3$	**L3**	^{t}Bu	**R-5**	Monomeric
-$SiMe_2Ph$	**L4**	^{i}Pr	**R-6**	Aggregated[a]
-$SiMe_2Ph$	**L4**	^{t}Bu	**R-7**	Monomeric
-$SiMePh_2$	**L5**	Et	**R-8**	Aggregated
-$SiMePh_2$	**L5**	^{i}Pr	**R-9**	Monomeric
-$SiPh_3$	**L6**	Et	**R-10**	Monomeric

[a]Slightly aggregation, indicated by the well-resoved methine resonance and small featureless methyl resonance peaks in ^{1}H NMR spectrum.

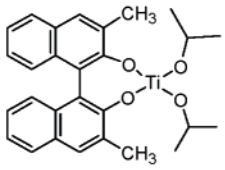

R-11

Recently, we reported our preliminary results on the helix-sense-selective polymerization of achiral carbodiimides using [(*R*)- and/or (*S*)-binaphthoxy](diisopropoxy)titanium(IV), **R-1** and/or **S-1**, catalysts (Scheme 1).[8] However, the helical polyguanidines obtained possess regioirregular backbones. We concluded that it is resulted from the multiple catalytically active species, such as monomer, dimers, and trimers of titanium complexes.[9] To precisely control the regioselectivity in the polymerization of unsymmetrical carbodiimides, structurally well-defined monomeric titanium catalysts are required. However, to date, monomeric titanium alkoxide complexes are few in number.

In the present study, we pursued two approaches to prevent the d^0 Ti(IV) aggregation and increase its reactivity by introducing bulky and electron-withdrawing groups onto the 3,3′-positions of naphthalene rings, and tuning the bulkiness of alkoxy groups. Among the titanium complexes synthesized, [(*R*)-3,3′-dibromo-2,2′-binaphthoxy](di-*tert*-butoxy)titanium(IV), **R-3** (Scheme 1), exists as a dimer in the solid state and a monomer in the solution state at room temperature. Catalyzed by **R-3**, helix-sense-selective polymerization of achiral carbodiimide of *N*-(1-anthryl)-*N*′-octadecylcarbodiimide (**1**) yielded poly-**1b** with high regioregularity, stereoselectivity and a relatively narrow molecular-weight distribution of 2.7. Although poly-**1b** possesses no chiral moieties in the polymer chains, this material exhibits thermo-driven and solvent-driven reversible chiroptical switching phenomena.

Results and Discussion

Chiral titanium complexes were synthesized from (*R*)-2,2′-binaphthoxy ligands (**L1**−**L6**) with an equivalent of the corresponding Ti(IV) alkoxide in toluene or benzene (Scheme 1). Complexation rates of these ligands are retarded from **L1** to **L6**, probably due to steric effects. For example, reacting bulky bis(triphenylsilyl) substituted ligand, **L6**, with $Ti(OEt)_4$ in refluxing toluene for a day yielded a mixture of **R-10** and the starting material **L6**, as evidenced by the remaining resonance peak at 4.64 ppm (−OH) in the ^{1}H NMR spectrum. In contrast, the reaction of the parent ligand, **L1**, with $Ti(O\text{-}i\text{-}Pr)_4$ or $Ti(O\text{-}t\text{-}Bu)_4$ at room temperature was complete within 1 h. **R-10** is monomeric, as evidenced by its light yellow color in solution and the single set of well-resolved quadruplet resonance peaks at 3.25 ppm ($-OCH_2CH_3$) in the ^{1}H NMR spectrum (see Supporting Information). The less bulky bis(diphenylmethylsilyl) substituted ligand, **L5**, gave monomeric **R-9** having bulkier isopropoxide groups, but aggregated, **R-8**, with the less bulky ethoxide groups, indicated by the featureless alkyl-H resonance peaks in the ^{1}H NMR spectrum and the red-orange color in solutions. This reveals that the bulkiness of R_2 also plays an important role in determining the existing forms of the titanium complexes. Complexes **R-4** and **R-6** possessing the isopropoxide groups exist in aggregated forms in solution, but using the more bulky *tert*-butoxide groups leads to monomeric **R-5** and **R-7** with ligands **L3** and **L4**. The light yellow color of **R-3** solutions indicates that **R-3** exists as a monomer. Parent ligand **L1** produced aggregated **R-1** and **R-2** with red-orange colors.

Preliminary polymerization experiments were carried out to test the activity of these monomeric titanium catalysts. The bromo substituted catalyst **R-3** shows the highest polymerization activity as compared to other monomeric complexes. This rate enhancement can be explained by both steric effects and the electron-withdrawing character of the brominated binaphthol ligand. In the following study, we therefore focused on the new catalyst, **R-3**.

The X-ray-quality single crystals were grown by extremely slow diffusion of a nonsolvent, acetonitrile, into methylene chloride solution of **R-3**. As shown in Figure 1, **R-3** exists as a dimer with a crystallographic C_2 symmetry in solid, in which the naphthylate oxygens are bridging the titanium centers, and the *t*-BuO alkoxides are all terminal. The coordination environ-

(7) For polyisocyanides: (a) Deming, T. J.; Novak, B. M. *J. Am. Chem. Soc.* **1992**, *114*, 7926. (b) Nolte, R. J. M.; van Beijnen, A. J. M.; Drenth, W. *J. Am. Chem. Soc.* **1974**, *96*, 5932. (c) Kamer, P. C. J.; Nolte, R. J. M.; van Beijnen, A. J. M.; Drenth, W. *J. Am. Chem. Soc.* **1988**, *110*, 6818. For poly(quinoxaline-2,3-diyl)s: (d) Ito, Y.; Miyake, T.; Ohara, T.; Suginome, M. *Macromolecules* **1998**, *31*, 1697. (e) Ito, Y.; Ihara, M.; Murakami, M. *Angew. Chem., Int. Ed. Engl.* **1992**, *31*, 1509. For poly(trityl methacrylates): (f) Nakano, T.; Okamoto, Y. *Macromolecules* **1999**, *32*, 2391. (g) Okamoto, Y.; Suzuki, K.; Ohta, K.; Hatada, K.; Yuki, H. *J. Am. Chem. Soc.* **1979**, *101*, 4763. (h) Nakano, T.; Okamoto, Y.; Hatada, K. *J. Am. Chem. Soc.* **1992**, *114*, 1318. For poly(trityl methacylamides): (i) Hoshikawa, N.; Hotta, Y.; Okamoto, Y. *J. Am. Chem. Soc.* **2003**, *125*, 12380. For polyacetylenes: (j) Aoki, T.; Kaneko, T.; Maruyama, N.; Sumi, A.; Takahashi, M.; Sato, T.; Teraguchi, M. *J. Am. Chem. Soc.* **2003**, *125*, 6346. For polyisocyanates: (k) Okamoto, Y.; Matsuda, M.; Nakano, T.; Yashima, E. *Polym. J.* **1993**, *25*, 391.

(8) (a) Tang, H.-Z.; Lu, Y.; Tian, G.; Capracotta, M. D.; Novak, B. M. *J. Am. Chem. Soc.* **2004**, *126*, 3722. (b) Tian, G.; Lu, Y.; Novak, B. M. *J. Am. Chem. Soc.* **2004**, *126*, 4082.

(9) (a) Boyle, T. J.; Barnes, D. L.; Heppert, J. A.; Morales, L.; Takusagawa, F. *Organometallics* **1992**, *11*, 1112. (b) Balsells, J.; Davis, T. J.; Carroll, P.; Walsh, P. J. *J. Am. Chem. Soc.* **2002**, *124*, 10336. (c) Davis, T. J.; Balsells, J.; Carroll, P. J.; Walsh, P. J. *Org. Lett.* **2001**, *3*, 699. (d) Pescitelli, G.; Di Bari, L.; Salvadori, P. *Organomettallics* **2004**, *23*, 4223.

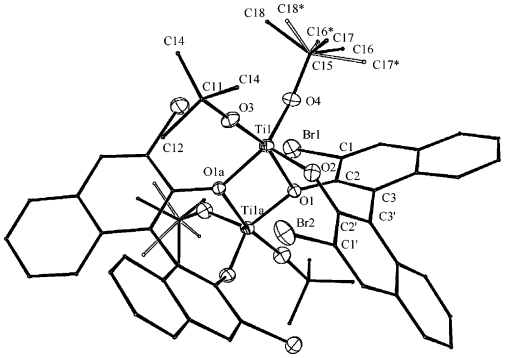

Figure 1. X-ray crystal structure of **R-3**. Crystal data: 0.42 × 0.30 × 0.28 mm, hexagonal, $P6_4$, $a = 21.190(5)$ Å, $c = 11.783(2)$ Å, V = 4583.4(17) Å^3, $Z = 6$, $d_c = 1.475$ g cm^{-3}, $\lambda = 0.71073$ Å, $2\theta_{max} = 55.8°$, $F(000) = 2047.11$, $T = 125$ °C. Selected bond distances and angles are found in Table 1.

Table 1. Selected Intramolecular Bond Distances (A) and Angles (deg) in **R-3** and **R-11**[a]

	R-3	R-11
O1−Ti1	2.175(3)	2.128(7)
O2−Ti1	1.851(4)	1.827(7)
O3−Ti1	1.750(4)	1.741(9)
O4−Ti1	1.782(4)	1.771(8)
O1a−Ti1	1.996(3)	1.953(7)
O1a−Ti1−O1	69.03(13)	69.5(2)
O1a−Ti1−O2	114.86(17)	124.6(3)
O1a−Ti1−O3	95.66(16)	94.7(3)
O1a−Ti1−O4	127.39(17)	117.9(3)
O2−Ti1−O4	108.87(18)	110.2(4)
O2−Ti1−O3	98.84(18)	100.9(4)
O3−Ti1−O4	105.25(19)	102.0(5)
Ti1−O1a−Ti1a	110.78(15)	109.9(3)
Ti1−O1−Ti1a	110.78(15)	110.6(3)
C2−C3−C3′-C2′	−56.8(7)	

[a] The data of **R-11** are taken from ref 9a.

ment about each titanium center is best described as a highly distorted trigonal bipyramid, with a bridging naphtholate (i.e., O1a) ligand and one *t*-BuO (i.e., O4) ligand occupying the axial positions with respect to titanium, and one *t*-BuO (i.e., O3), a terminal naphtholate (i.e., O2) and a bridging naphtholate (i.e., O1) ligand occupying the remaining equatorial sites. This structure is quite similar to the dimer of **R-11** [(*R*)-3,3′-dimethyl-2,2′-binaphthoxy](diisopropoxy)titanium(IV)] (Scheme 1).[9a] As listed in Table 1, Ti−O-*t*-Bu distances are nearly 0.1 Å shorter than Ti−ONp distances, revealing that the bonds between Ti−O-*t*-Bu are stronger due to the greater electron rich character of the oxygen of the −O-*t*-Bu group. Meanwhile, compared to the dimer of **R-11**, three significant differences are found: (1) The two −O-*t*-Bu groups in **R-3** are in different environments; one is confined, but another has two orientations. (2) The dimer of **R-3** displays an exact crystallographic C_2 symmetry, whereas the dimer of **R-11** has a slight puckering of 1,3-dioxadititanacycle and shows virtual C_2 symmetry. (3) All the Ti−O distances in **R-3** are longer (0.01−0.05 Å) than those in **R-11** (Table 1), revealing that **R-3** occupies a larger space due to the overall more crowded environment in **R-3**.

Figure 2 shows the variable-temperature ^{1}H NMR spectra in the aromatic regions of **R-3** in CD_2Cl_2. When the temperature was lowered, the well-resolved resonance peaks observed at −40 °C were broadened at −50 °C, and new resonance peaks appeared below −60 °C. These results are interpreted as **R-3**

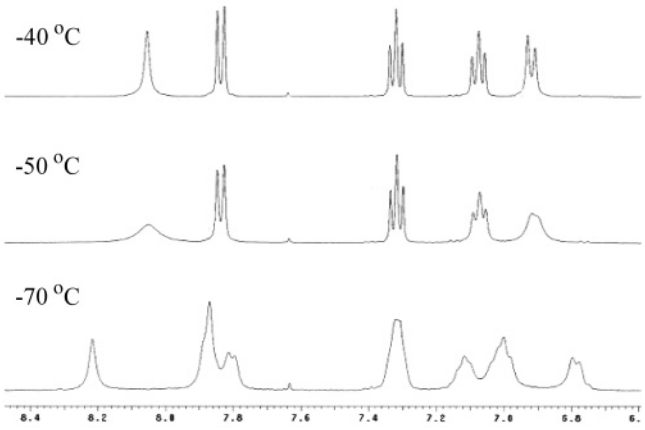

Figure 2. Variable-temperature ^{1}H NMR spectra of **R-3** in CD_2Cl_2.

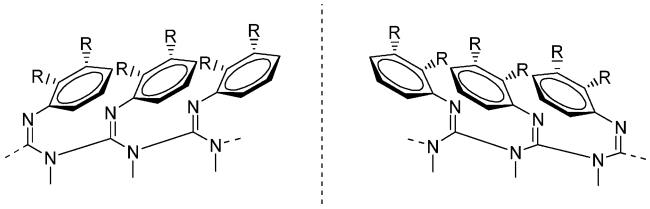

Figure 3. Stereoregular structures of non-symmetrically substituted polyguanidines prepared through the polymerization of an achiral carbodiimide with catalyst **R-1**.

existing as a monomer above −50 °C but a monomer and dimer mixture below −60 °C. This equilibrium is also supported by the single methyl resonance peak at 1.02 ppm above −50 °C and a split peak below −60 °C. This NMR study strongly supports the previous conclusion of the monomeric nature of **R-3** that was based on the observation of the light yellow color of **R-3** in solution.

We previously reported that **R-1** and **S-1** catalysts will polymerize achiral, but non-symmetrically substituted carbodiimides (e.g., *N*-(1-isopropyl-6-methylphenyl)-*N*′-methylcarbodiimide (**2**)) to yield helix-sense-selective polymers that do not fully racemize through helix inversions upon annealing.[8b] We attribute this unusual behavior to a second level of embedded chirality that results from the stereoselective orientation of both the aromatic substituents and the imine groups (Figure 3). Full racemization of these stereoregular structures requires not only helix reversals but rotations around the N-aryl bonds and/or inversion of the imine nitrogens. Because of steric interactions between neighboring groups, these normally low energy processes are strongly inhibited.

Catalyzed by **R-3**, helical poly-**1b** was obtained by polymerization of **1** in toluene at room temperature (Scheme 2). Both poly-**1a** and poly-**1b** show high solubility in toluene, chloroform, and tetrahydrofuran (THF). As shown in Figure 4, compared to poly-**1a** ($M_w = 234\,000$, PDI = 19.3), poly-**1b** ($M_w = 16\,000$) has much narrower polymer dispersion index, PDI = 2.7, indicating that the single site catalyst **R-3** offers superior control over the polymerization. Furthermore, contrary to the regioirregular polymer structure of poly-**1a**, poly-**1b** has a well-defined regioregular backbone as evidenced by the single C═N stretching at 1642 cm^{-1} in FT-IR spectrum (See Supporting Information).

The C_2 symmetric titanium catalyst possesses two different Ti−O bonds of Ti−OR_2 (**a**) and Ti−ONp (**b**). Based on the

Scheme 2

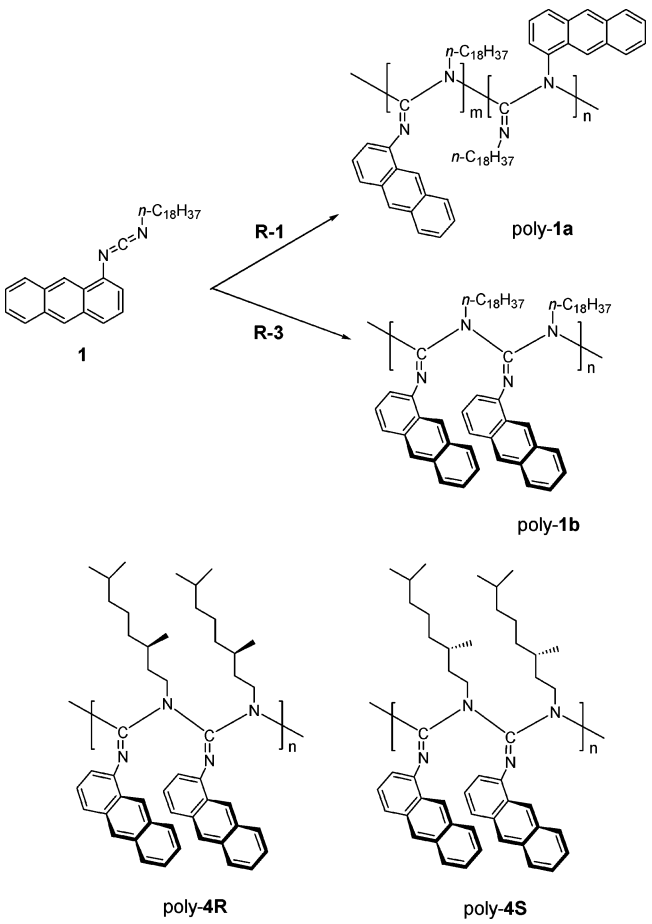

previously proposed mechanism,[10] bond **a** or **b** selectively inserts into a carbodiimide and R_2O- or NpO− becomes the end group of the polymer chain. In this competition, the nucleophilicity of $-OR_2$ is greater than −ONp due to its greater electron-rich character of its oxygen. Once completed, the polymerization is quenched and the titanium alkoxide endgroup is protonolysis removed from the amidinate chain end using methanol. This mechanism predicts that the achiral R_2O- not the chiral NpO− is the end groups in the helical polyguanidines. To confirm this, we carried out the polymerization of *N*,*N*′-dihexylcarbodiimide (**3**) catalyzed by **R-1** (the molar ratio of [**3**]/[**R-1**] is 5), and found that Ar−H resonance peaks completely (i.e., the residual chiral catalyst) disappeared after the purification by reprecipitation of the polymer solution in THF or chloroform into methanol. It demonstrates that no chiral binaphthyl groups remain in the resulting polyguanidines.

Figure 5 shows the optical rotations, $[\alpha]^{80}_D$, of poly-**1a** and poly-**1b** in toluene at 80 °C versus annealing time. Compared to poly-**1a**, the initial $[\alpha]^{80}_D$, −560°, of poly-**1b** is much greater in intensity indicative of greater diastereoselectivity but opposite in sign. The racemization rate ($t_{1/2}$) for poly-**1b** is 27 h, 6 times longer than that of poly-**1a**. It is worth pointing out the racemization rate of poly-**1b** is the slowest of all the polyguanidines measured to date.

This experiment, however, leads to a puzzle. Why is it that poly-**1b** and poly-**1a** show optical rotations of opposite sign in toluene at +80 °C? To explore this, we measured the optical rotations of poly-**1b** at different temperatures. The first observation is that these polymers show a drastic temperature dependence in their optical rotations both in terms of magnitude and sign. As shown in Figure 6, $[\alpha]_D$ of poly-**1b** converts its sign from positive (e.g., $[\alpha]^{31}_D = +300°$) at lower temperature to negative ones (e.g., $[\alpha]^{44}_D = -205°$) at higher temperature. The chiroptical switching temperature is 38.5 °C. As reported previously,[8a] $[\alpha]^{20}_D$ of poly-**1b** in toluene is +130°. Both positively signed optical rotations of poly-**1a** and poly-**1b** at lower temperatures indicate that the same *M*-conformations of **R-1** and **R-3** give the same preferred screw-sense polymers at the polymerization conditions.

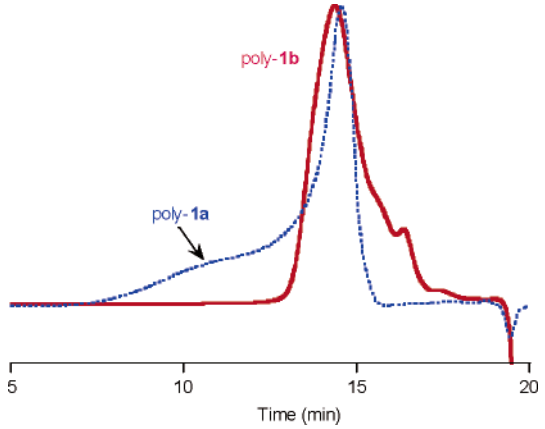

Figure 4. GPC chromatograms of poly-**1a** and poly-**1b** eluting with chloroform at a rate of 1.0 mL/min.

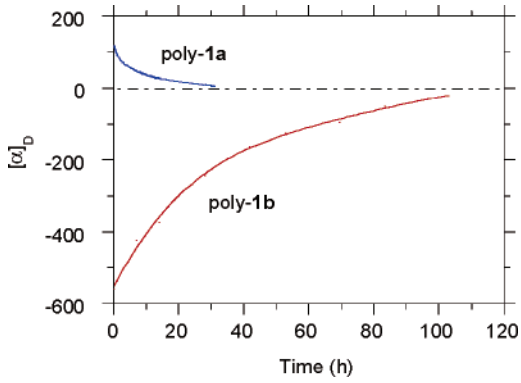

Figure 5. Optical rotations, $[\alpha]_D$, of poly-**1a** and poly-**1b** versus annealing time in toluene at 80 °C (c = 0.1 g/100 mL).

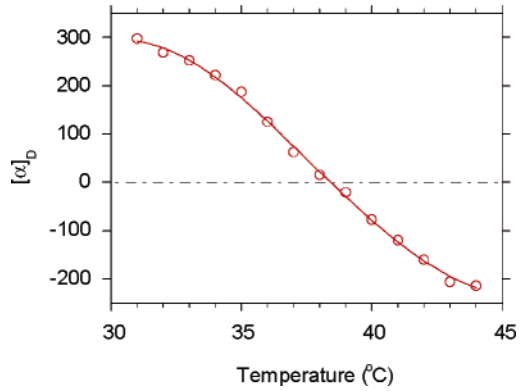

Figure 6. Variable-temperature $[\alpha]_D$ of poly-**1b** in toluene (c = 0.1 g/100 mL) at a heating rate of 1.5 °C/min.

(10) Shibayama, K.; Seidel, S. W.; Novak, B. M. *Macromolecules* **1997**, *30*, 3159.

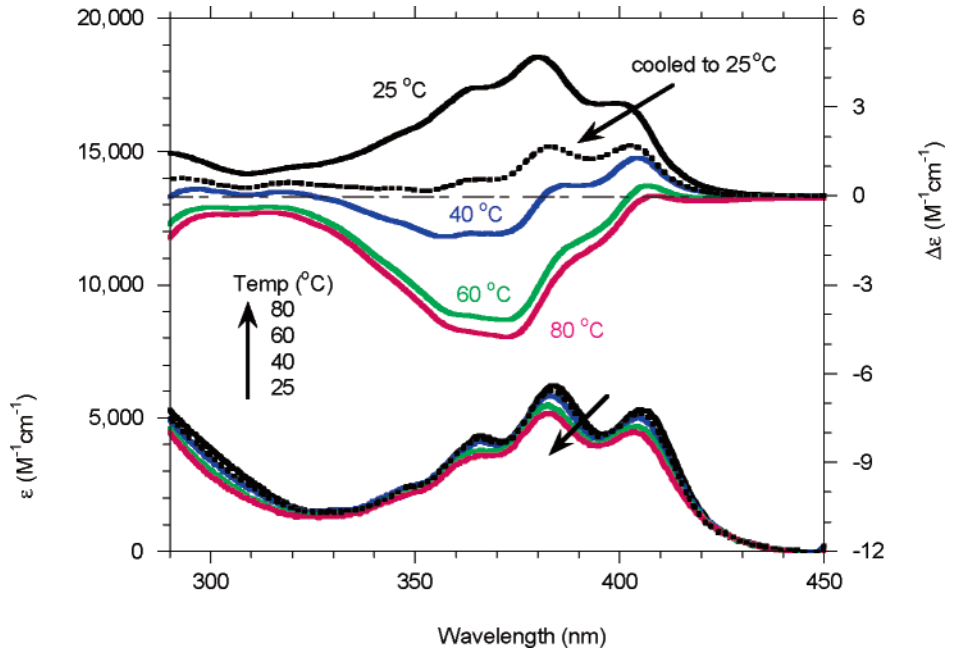

Figure 7. Variable-temperature CD (top) and UV−visible (bottom) spectra of poly-**1b** in toluene ($c = 2.1 \times 10^{-4}$ M, path length = 10 mm).

To further understand the chiroptical switching phenomenon, variable temperature CD and UV−visible spectra were recorded (Figure 7). At 25 °C, poly-**1b** shows a positively signed Cotton effect with the maximum $\Delta\epsilon = +4.69$ M^{-1} cm^{-1} at 380 nm, corresponding to the UV−visible absorption maximum at 384 nm. The Kuhn's dissymmetry ratio, g_{abs} ($= \Delta\epsilon/\epsilon$), is $+8.2 \times 10^{-4}$, comparable to that ($+14.2 \times 10^{-4}$) of the stable helical poly{*N*-(1-anthryl)-*N*′-[(*R*)-3,7-dimethyloctyl]guanidine} (poly-**4R**, Scheme 2). When poly-**1b** was heated in a toluene solution, it showed a weak Cotton effect at 40 °C, but gave an almost mirror-image Cotton effect at higher temperature with that at room temperature; and the UV−visible absorption decreased slightly. For example, at 80 °C, poly-**1b** gave a negatively signed Cotton effect with maximum $\Delta\epsilon = -4.69$ M^{-1} cm^{-1} at 372 nm, corresponding to the maximum UV−visible absorption at 382 nm. g_{abs}, is -12.7×10^{-4}, comparable to that (-11.0×10^{-4}) of the stable helical poly{*N*-(1-anthryl)-*N*′-[(*S*)-3,7-dimethyloctyl]guanidine} (poly-**4S**, Scheme 2) in toluene at 80 °C. The most interesting observation is that when this toluene solution was cooled to 25 °C, once again poly-**1b** gave a positively signed Cotton effect albeit with lower intensity compared to the original one at 25 °C. This reveals that the chiroptical properties of helical poly-**1b** can be reversible switched around 40 °C without racemizing the polymer. The decrease in the intensity is due to slow racemization during the entire thermal process.

Keeping in mind the fact of slow racemization in toluene at 80 °C, we further performed the heating−cooling cycles of poly-**1b** in toluene in the temperature range of 25 °C and 60 °C. As expected, no significant racemization was observed. Poly-**1b** shows absolutely reversible chiroptical switching in the four thermal cycles as we conducted. Figure 8 displays the CD and UV−visible spectra of poly-**1b** in toluene in the first two heating−cooling cycles.

Figure 9 shows the variable temperature CD and UV−visible spectra of poly-**1b** in chloroform. When the temperature was raised from 25 °C to 60 °C, slight decrease in the UV−visible absorption was observed. However, the g_{abs}-values remained constant. Figure 10 shows the variable temperature CD spectra of poly-**1b** in tetrahydrofuran (THF). Slight increase in the absolute g_{abs}-values was observed.

Interestingly, poly-**1b** shows negative Cotton effects in chloroform and THF at all temperatures. These CD spectra resemble that of poly-**1b** in toluene at 60 °C, but are of opposite in sign, compared to that of poly-**1b** in toluene at 25 °C. This indicates the solvent-driven chiroptical switching. Figure 11, which shows the solvent-composition dependence of the g_{abs}-values of poly-**1b**, clearly demonstrates the chiroptical inversion driven by the change in solvent composition between toluene and THF. The chiroptical inversion occurs around 10% content of THF.

Scheme 3 shows the possible molecular motions leading to the full racemization of poly-**1b**. They are the N−C bond rotations (ϕ) in the backbone, N−C_{Ar} bond rotations (θ) in the side chains, and the imine configuration interconversions (ω). ϕ is related to the torsion angle of the main chains, which determines the helical screw sense and the helical pitches. The helical inversion barrier of poly-**1b** is unknown, though we attempted to calculate it theoretically using polymer-consistent-force-field (pcff). The barrier for a structural analogue of polyguanidines, polyisocyanates, was estimated as 12.5 kcal/mol by an empirical force field.[11] Considering the stiffer backbone of the polyguanidine, it is reasonable to assume that the helical inversion barrier of poly-**1b** is greater than 12.5 kcal/mol. Pcff calculations reveal a limited rotation between N−C_{Ar} ($0 < \theta < 90°$) because of the great bulkiness of anthracene groups, indicating that the energy for the free rotations are extremely high but a low energy for the limited reorientation (wagging) of the anthracence rings. The barrier of imine configuration interconversions in small molecules is in the range of 20−26 kcal/mol (coalescence temperatures in the range of 50−180 °C).[12] Thus, the energy barrier in poly-**1b** is probably in the sequence of $\Delta E(\omega) > \Delta E(\phi) > \Delta E(\theta)$. The full

(11) Lifson, S.; Felder, C. E.; Green, M. M. *Macromolecules* **1992**, *25*, 4142.
(12) Jennings, W. B.; Boyd, D. R. *J. Am. Chem. Soc.* **1972**, *94*, 7187.

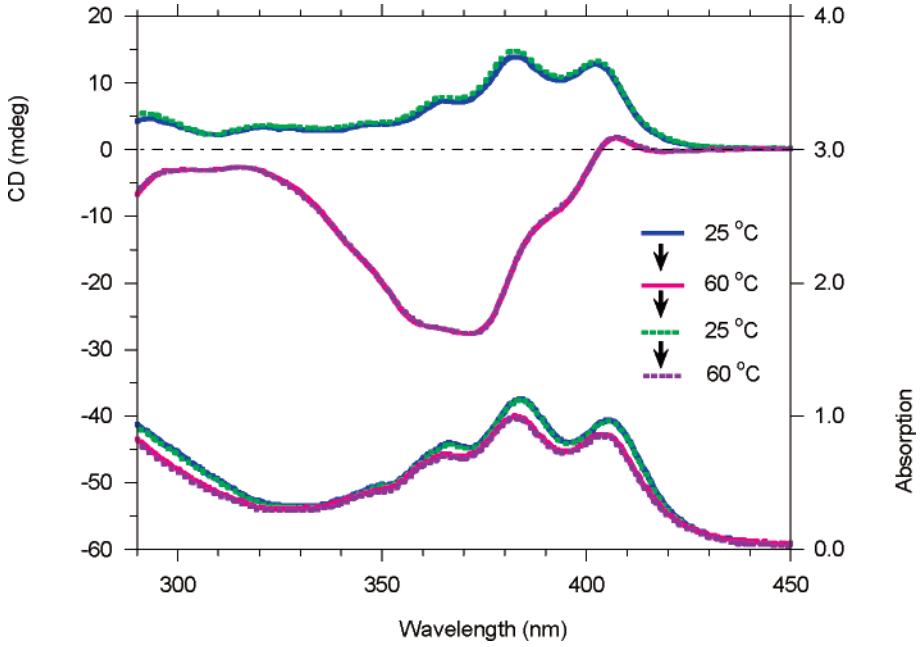

Figure 8. Variable-temperature CD (top) and UV−visible (bottom) spectra of poly-**1b** in toluene ($c = 2.1 \times 10^{-4}$ M, path length = 10 mm) in the heating−cooling−heating thermal cycle. The sample is the same as that in Figure 7. The measurement was performed six month later compared to that in Figure 7.

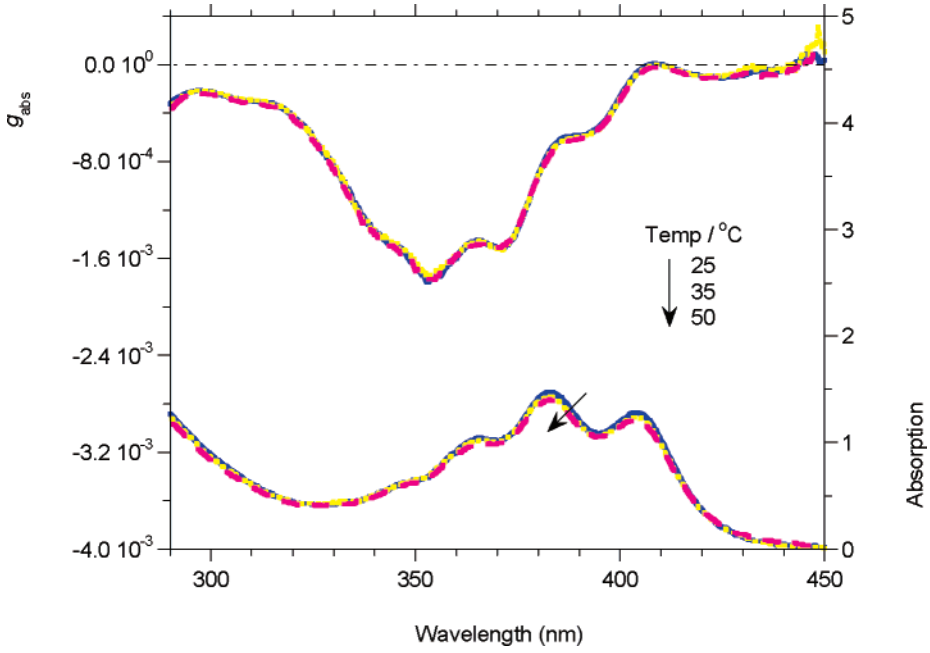

Figure 9. Variable-temperature g_{abs} (top) and UV−visible (bottom) spectra of poly-**1b** in chloroform ($c = 2.1 \times 10^{-4}$ M, path length = 10 mm).

racemization of poly-**1b** occurring at +80 °C takes more than 100 h, and probably results from contributions by all three of these processes.

Three mechanisms are possible to explain this interesting chiroptical switching phenomenon: helix inversions, imine inversions and/or rotations around the N-anthracene bonds. Of the three, partial rotations (wagging) around the N-anthracene bonds are the lowest energy process. Compared to the time-consuming (100 h) and energy-demanding (+80 °C) full racemization process, the reversible chiroptical inversion occurs quickly (less than 1 min) by themo-driven at the lower temperature of +38.5 °C in toluene and by changes in solvent polarity, implying that the imine configuration inversion and the helix inversion in poly-**1a** are not involved in this reversible chiroptical switching process. The blue-red shift in UV−visible and CD absorptions above and below the chiroptical switching temperature, however, suggest that the directions of the anthracence rings cooperatively switch relative to the helix director (i.e., wagging in θ around the N−C_{Ar} bond). The helical pitches in these various states may also vary in this process. Hence, although small contributions from helical reversals and imine inversions cannot be ruled out, we believe that changes in the helical pitches and the directions of the transition dipole moments of anthracence may lead to this chiroptical switching phenomenon.[13] The clear reversible switching mechanisms are under study.

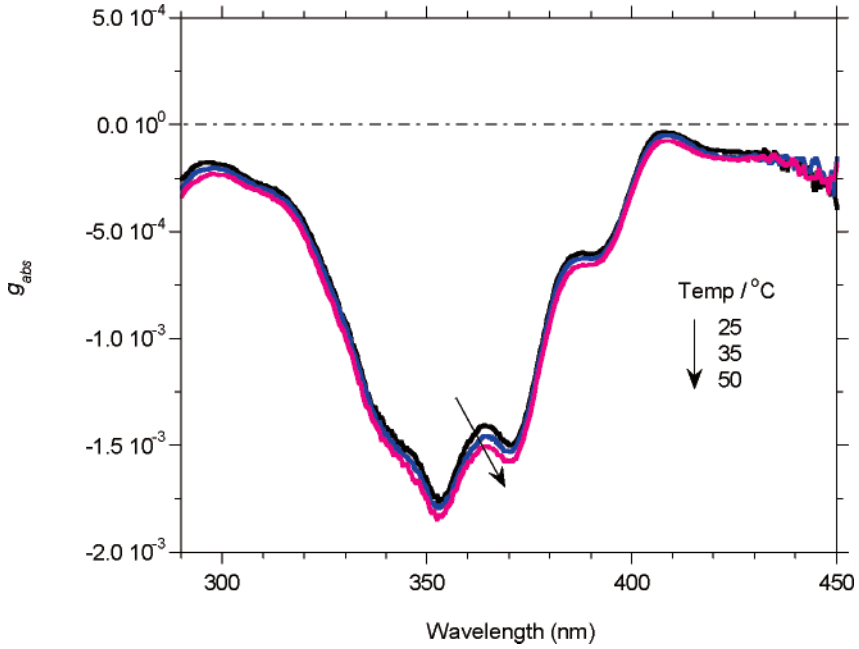

Figure 10. Variable-temperature g_{abs} spectra of poly-**1b** in THF ($c = 2.1 \times 10^{-4}$ M, path length = 10 mm).

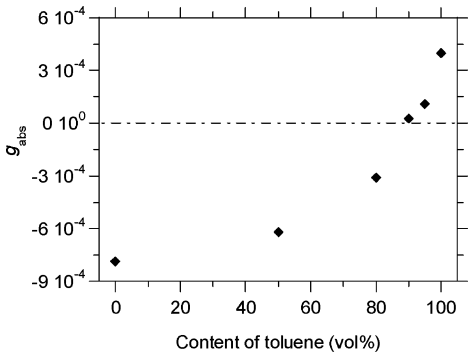

Figure 11. g_{abs}-values at 380 nm of poly-**1b** in toluene/THF at 25 °C.

Scheme 3

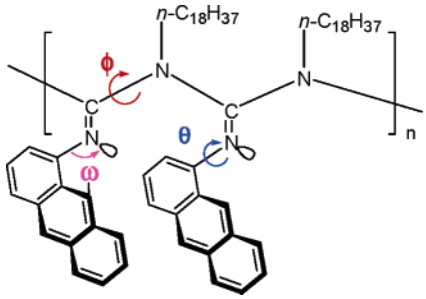

Concluding Remarks

We have synthesized a series of chiral binaphthyl titanium complexes for use in helix-sense-selective polymerizations. Among them, chiral titanium complex **R-3** exists as a crystallographic C_2 dimer in solid but a monomer in solution at room temperature. Application of **R-3** in the helix-sense-selective polymerization of achiral carbodiimide **1** yielded a well-defined regioregular, stereoregular poly-**1b** with a relatively narrow PDI of 2.7. Poly-**1b** was found to undergo dramatic reversible chiroptical switching that is extremely sensitive and can be driven by heat and solvent polarity. Chiroptical switching occurs at 38.5 °C in toluene and around 10% THF content in mixed THF/toluene at 25 °C. This is the first example of chiroptical switching occurring in a helical polymer possessing no chiral moieties in the polymer chains, and may prove useful in low-cost optical memory and switching applications. The reversible chiroptical switching occurs at substantially lower energy than racemization (>100 h, +80 °C). After evaluating the potential motions that may be behind this switching phenomenon, we believe the reversible chiroptical switching phenomenon occurs by a cooperative switching of the orientation of the anthracene rings. It remains an open question as to whether helical and/or imine inversions play a role in this process. The clear mechanism are under detailed study.

Acknowledgment. We thank Professors A. Clay Clark, T. Brent Gunnone, and Alan E. Tonelli at NCSU for use of their CD and FT-IR instruments and the Silicon Graphics Indigo II XZ computing system. We appreciate Professors Alan E. Tonelli, Stefan Franzen, Dr. Xingwu Wang, and Xin Jia for their help and discussion on the pcff calculations. We also thank Jubo Zhang for his help in the preparation of the X-ray crystals.

Supporting Information Available: All experimental details and crystallographic data for **R-3** (PDF, CIF). This material is available free of charge via the Internet at http://pubs.acs.org.

JA0453533

(13) Tinoco, I. *J. Chim. Phys.* **1968**, *65*, 91.
(14) (a) Tsang, W. C. P.; Schrock, R. R.; Hoveyda, A. H. *Organometallics* **2001**, *20*, 5658. (b) Maruoka, K.; Itoh, T.; Araki, Y.; Shirasaka, T.; Yamamoto, H. *Bull. Chem. Soc. Jpn.* **1988**, *61*, 2975. (c) Ooi, T.; Kameda, M.; Maruoka, K. *J. Am. Chem. Soc.* **2003**, *125*, 5139. (d) van der Linden, A.; Schaverien, C. J.; Meijboom, N.; Ganter, C.; Orpen, A. G. *J. Am. Chem. Soc.* **1995**, *117*, 3008.